



Possible reaction pathways of the lincomycin molecule according to the DFT calculation method

BAHAR EREN¹ and YELDA YALCIN GURKAN^{2*}

¹Namik Kemal University, Faculty of Agriculture, Tekirdag, Turkey and ²Namik Kemal University, Department of Chemistry, Tekirdag, Turkey

(Received 21 July, revised 21 October, accepted 8 November 2016)

Abstract: Human-used antibiotics are eliminated from the body with little or no transformation at all. Traces of eliminated antibiotics enter the receiving environment directly since they cannot be treated in prevalent wastewater treatment facilities. Thus, wastewaters containing traces of antibiotics have to be treated accordingly. Lincomycin is subsequently isolated from *Streptomyces lincolnensis*. Lincomycin and its derivatives are antibiotics exhibiting biological activity against Gram-positive bacteria, and are natural antibiotics in the environment as pollutants. This study aims to predict the degradation mechanism of lincomycin molecule in the gaseous phase and aqueous media. Probable reaction path of lincomycin molecule with OH radicals was analyzed. Optimized geometry was calculated via Gauss View 5. Subsequently, the lowest energy status was determined through geometric optimization via Gaussian 09 program. Aiming to determine the intermediates in photocatalytic degradation mechanism of lincomycin, geometric optimization of the molecule was realized through DFT method. Activation energy for the probable reaction path was calculated, and their most stable state from the thermodynamic perspective determined for the gaseous phase and aqueous media. Impact of water solvent was investigated using the conductor-like screening solvation model (COSMO). The predicted mechanism was confirmed by comparison with experimental results on simple structures reported in literature.

Keywords: lincomycin; hydroxyl radical; DFT; COSMO; Gaussian 09.

INTRODUCTION

Demand for antibiotics in the world is growing continuously. The threat of infectious diseases has been considerably decreased through antibiotics since their discovery in the 20th century. Deaths from diseases that were once prevalent and fatal decreased dramatically through the combination of the so-called “miracle drugs” and improvements in sanitation, housing, food, and the occurrence of

* Corresponding author. E-mail: yyalcin@nku.edu.tr
doi: 10.2298/JSC160721102E

mass immunization programmes. For many years, the lives of millions of people were saved and their sufferings were reduced *via* antibiotics. In the late 20th century, antibiotics not only have saved peoples lives, but also increased life expectancy.¹

There are various ways for active pharmaceutical ingredients to enter the environment. The cycle starts with human beings and animals, ends up in wastewater, soil, groundwater, and finally, if not treated properly, it arrives at potable water supplies. Due to the long half-life of antibiotics, some of the antibiotics reaching the environment can be found in nature. In wastewater treatment facilities, active components are released into the environment with almost no change. In the case that metabolites are still biologically active, aqueous organisms in the environment are affected, and consequently these become a threat not only to the ecosystem, but also to human beings.²⁻⁴

Due to their designed effect, antibiotics primarily affect organisms such as bacteria, fungi and microalgae. Antibiotics are discharged into the environment with a slight or no change, and conjugate to polar molecules.⁵ Antibiotics accumulate in different environmental compartments because of their low biodegradability.⁶ Natural cycles, products, production facilities, and soil are the resources of antibiotics in nature. In terms of risk assessment of antibiotics, natural concentrations of them are important for the natural cycle. Some of the antibiotics produced from soil bacteria are beta lactam antibiotics; there are streptomycins and aminoglycosides as well. Streptomyces is one of the soil bacteria within the actinomycetes group. Thus, antibiotics are produced by streptomycete bacteria.¹

The action and behaviour of antibiotics is an important issue in environmental chemistry. The amount of antibiotics used for veterinary purposes and for manuring land is estimated to be more than one kg per ha. In addition, antimicrobial agents used for animals can be discharged into the environment from agricultural lands.⁷⁻¹³

Because of their changeable steric genus, antibiotics are ionized as amphiphilic or amphoteric, thus allowing the adsorption to take place in soil.⁷ Because of the physical and chemical properties, such as molecule size, solubility, hydrophobicity, sorption and fixation of agents, there is a difference in antibiotic interaction with soil. Many agents are obstructed strongly in soil due to their being polar and slowly soluble in water.¹⁴

Organic contaminants exist at very low concentrations in water.¹⁵ Therefore, it is essential that the organic contaminants be removed from drinking water.¹⁶ Natural purification of water systems such as rivers, creeks, lakes, and pools is realized by solar light on earth. Sunbeams initiate the degradation reaction of large organic molecules into smaller basic molecules, finally providing the formation of CO₂, H₂O and other molecules.^{17,18}

In its reactions with organic molecules, $\cdot\text{OH}$ behaves as an electrophile whereas $\text{O}^\cdot-$ is a nucleophile. Thus, $\cdot\text{OH}$ readily adds to unsaturated bonds while $\text{O}^\cdot-$ does not. Both forms of the radical abstract H from C–H bonds and this can result in the formation of different products when the pH is raised to a range where $\text{O}^\cdot-$ rather than $\cdot\text{OH}$ is the reactant. For example, if an aromatic molecule carries an aliphatic side chain, $\text{O}^\cdot-$ attacks there by H abstraction whilst $\cdot\text{OH}$ adds preferentially to the aromatic ring.¹⁹ Hydroxyl radical which is the most reactive type known in biological systems reacts with every biomolecule it encounters including water. Potentially, every biomolecule is a hydroxyl radical scavenger but at different speeds.²⁰ Aromatic compounds are good detectors since they can be hydroxylated. In addition, the position of attack to the ring depends on the electron withdrawal and repulsion of previously present substituents. The attack of an aromatic compound by any hydroxyl radical results in the formation of a hydroxylated product.²¹

This study aims to predict the degradation mechanism of the lincomycin molecule in the gaseous phase and in aqueous media. The probable reaction path of lincomycin molecule with $\cdot\text{OH}$ was analysed through the density functional theory (DFT) method.

COMPUTATIONAL SET-UP AND METHODOLOGY

Computational models

The models of the molecules were formed by the use of the mean bond distances and the geometric parameters of the benzene ring. Tetrahedral angles were used for the sp^3 -hybridized carbon and oxygen atoms and 120° for the sp^2 -hybridized carbon atoms was used in the computational modelling. The aromatic ring was left planar, excluding the position of attack. Due to the change in the hybridization state of the carbon at the addition centre from sp^2 to sp^3 , the attacking $\cdot\text{OH}$ was presumed to create a tetrahedral angle with the C–H bond.²²

Molecular orbital calculations

In photocatalytic degradation reactions of lincomycin, it is possible that products more harmful than those in the original material could be formed. Therefore, before experimentally realizing a photocatalytic degradation reaction, it is essential to know the nature of the primary intermediate products. The most reliable and accurate information is gathered through calculations realized with quantum mechanical methods. Thus, since the yield produced was the same, photocatalytic degradation reactions of lincomycin and its hydroxy derivatives are based on the direct reaction of these molecules with $\cdot\text{OH}$.

With this aim, the kinetics of the reactions of lincomycin with $\cdot\text{OH}$ were theoretically analysed. The study was initiated with lincomycin and then exposed to reaction with $\cdot\text{OH}$ and the reaction yields were modelled in the gaseous phase. Experimental results in the scientific literature showed that $\cdot\text{OH}$ detach a hydrogen atom from saturated hydrocarbons, and $\cdot\text{OH}$ is added to unsaturated hydrocarbons and materials with this structure.²³ For this purpose, all possible reaction paths for the analysed reactions were determined. For every reaction path, molecular orbital calculations of the reactant, yield, transition state complexes were performed with the density functional theory (DFT) and their molecular orbital calculations were realized and their geometries optimized. In order to explore the conformational landscape of the

molecules, a potential energy surface scan was performed along the torsional coordinates mentioned above in a relaxed manner (*i.e.*, all other geometrical parameters were optimized at each point) for both conformers. The scan was calculated using the B3LYP/6-31G* method.²⁴

Kinetic data treatment

The aim of this study was to develop a model providing the outcome of the yield distributions of the photocatalytic degradation reactions. The vibration frequencies, the thermodynamic and electronic features of every structure were calculated using the obtained optimum geometric parameters. Subsequently, based on the quantum mechanical calculation results, the rate constant and activation energy (E_a) of every reaction was calculated at a temperature of 25 °C.

In order to enable the calculation of the rate constant, it is necessary initially to calculate the partition function of the activated complex. To realize this calculation, it is essential to know the geometry of the complex and the moments of inertia. In addition, E_a should be known in order to determine the rate constant. The activation energy, as the vibration frequency, can only be calculated quantum mechanically.

The most probable reaction path and the yield distribution of the reaction of $\cdot\text{OH}$ for every molecule were determined by comparing the obtained results. The optimized geometric structures were drawn *via* GaussView 5, and the calculations were realised within the Gaussian 09 programme packet.²⁵

Methodology

The investigated reaction system was composed of $\cdot\text{OH}$, which are open-shell species. It is known that open-shell molecules cause severe problems in quantum mechanical calculations. The self-consistent field method (SCF) calculation will proceed for an open-shell case in the same way as for a closed-shell case. However, since two sets of equations have to be dealt with, at each iteration, the program has to consider, either simultaneously or successively, the closed-shell and the open-shell equations. In this respect, the computational burden could be two-times larger for an open shell than that for a closed-shell. Another point raised in connection with the optimization of the SCF process for open-shell molecules is the relative intricacy of the sequence of calculations for the closed-shell Hamiltonian and the open-shell Hamiltonian.²⁶

Thus, DFT method with the Gaussian 09 programme was used in order to perform geometry optimization of the reactants, the product radicals, and the pre-reactive and transition state complexes.²⁵ DFT methods, taking the electron correlation into account, use the precise electron density to calculate molecular properties and energies. Spin contamination does not affect them and hence, for calculations involving open-shell systems, they become favourable. DFT calculations were made by the hybrid B3LYP functional combining the HF and Becke exchange terms with the Lee-Yang-Parr correlation functional.²²

It is essential in such calculations to choose the basis set. Based upon the obtained results, optimization in the current study was carried out at the B3LYP/6-31G(d) level. In the determination of the transition states, the forming C–O bonds in the addition paths and the H–O bond in the abstraction path were chosen as the reaction coordinates. By using frequency analyses at the same level, the ground state and transition state structures were approved. For the characterization of transition structures, one imaginary frequency that belonged to the reaction coordinate was set, subtending to a first-order saddle point. The zero-point vibrational energies (ZPEs) were measured at the B3LYP/6-31G(d) level.²²

Solvent effect model

The energetics of the degradation reactions of all organic compounds are affected by water molecules in aqueous media. In addition, geometry relaxation on the solutes is induced by H₂O. On the other hand, it was indicated in previous studies that there is an insignificant effect of geometry changes on the energy of the solute for both open- and closed-shell structures.²⁷ In this study, DFT/B3LYP/6-31+G(d) calculations were realised for the optimized structures of the reactants, the pre-reactive and the transition state complexes and the product radicals, by using the COSMO (conductor-like screening solvation model) as the solvation method in order to consider the effect of H₂O on the energetics and the kinetics of lincomycin + ·OH reactions. Water at 25 °C was used as a solvent with dielectric constant, $\epsilon = 78.39$.²⁸

The COSMO method explains the solvent reaction field through apparent polarization charges distributed on the cavity surface, determined by presuming that the total electrostatic potential cancels out at the surface. The solvation in polar liquids can be described by this condition. Therefore, this method was chosen to be appropriate for the present study.²⁸

RESULTS AND DISCUSSION

As seen in Table I, according to the analysis performed with the degradation method, the conformer with the lowest energy, *i.e.*, the most durable conformer of the lincomycin molecule, is the one obtained through the 2.2 pathway. In other words, degradation obtained through the 2.2 pathway is easiest, in the sense, of having the lowest energy path.

TABLE I. Energy, enthalpy, entropy and Gibbs energy changes (Ha) for the gaseous phase and aqueous phase of the degraded fragments of the lincomycin molecule

1.(Ha)	L0	L11	L12	L13	L14	L15	L16	L17
HF_G	-1664.76	-1546.80	-1296.74	-1183.40	-1128.05	-1129.26	-1089.95	-691.77
ΔE	-1664.21	-1546.34	-1296.41	-1183.08	-1127.75	-1128.94	-1089.668	-691.49
ΔH	-1664.21	-1546.34	-1296.41	-1183.08	-1127.75	-1128.94	-1089.66	-691.48
ΔG	-1664.30	-1546.420	-1296.48	-1183.15	-1127.82	-1129.01	-1089.72	-691.54
HF_S	-1664.76	-1546.81	-1296.76	-1183.42	-1128.07	-1129.27	-1089.95	-691.77
ΔE	-1664.20	-1546.35	-1296.43	-1183.10	-1127.78	-1128.95	-1089.67	-691.48
ΔH	-1664.20	-1546.35	-1296.43	-1183.10	-1127.77	-1128.95	-1089.67	-691.48
ΔG	-1664.29	-1546.43	-1296.50	-1183.16	-1127.84	-1129.02	-1089.73	-691.54
2.1.(Ha)	L0	L211	L212	L213	L214	L215	L17	
HF_G	-1664.76	-1625.44	-1227.26	-859.23	-745.90	-690.55	-691.77	
ΔE	-1664.21	-1624.92	-1226.75	-858.94	-745.61	-690.29	-691.49	
ΔH	-1664.21	-1624.92	-1226.74	-858.94	-745.61	-690.29	-691.48	
ΔG	-1664.30	-1625.01	-1226.83	-859.00	-745.67	-690.34	-691.54	
ΔH	-1664.20	-1624.92	-1226.74	-858.96	-745.63	-690.30	-691.48	
ΔG	-1664.29	-1625.01	-1226.83	-859.03	-745.69	-690.36	-691.54	
2.2.(Ha)	L0	L211	L222	L223	L224	L16	L17	
HF_S	-1664.75	-1625.44	-1227.26	-859.26	-745.92	-690.57	-691.77	
ΔE	-1664.20	-1624.92	-1226.74	-858.96	-745.63	-690.31	-691.48	
HF_G	-1664.76	-1625.44	-1257.42	-1144.08	-1088.73	-1089.95	-691.77	
ΔE	-1664.21	-1624.92	-1257.13	-1143.80	-1088.47	-1089.66	-691.49	
ΔH	-1664.21	-1624.92	-1257.13	-1143.80	-1088.47	-1089.66	-691.48	

TABLE I. Continued

2.2.(Ha)	L0	L211	L222	L223	L224	L16	L17
ΔG	-1664.30	-1625.01	-1257.19	-1143.86	-1088.53	-1089.72	-691.54
HF_S	-1664.75	-1625.44	-1257.44	-1144.10	-1088.75	-1089.95	-691.77
ΔE	-1664.20	-1624.92	-1257.15	-1143.81	-1088.49	-1089.67	-691.48
ΔH	-1664.20	-1624.92	-1257.15	-1143.81	-1088.49	-1089.67	-691.48
ΔG	-1664.29	-1625.01	-1257.21	-1143.87	-1088.55	-1089.73	-691.54

The probable degradation paths of lincomycin were determined to be N–C, C–S and C–O bond parts. Reaction centres can be explained through Mulliken charge distribution of the molecule. According to the data in Table II, the degradation reaction occurred due to the electronegativity of S, N, and O.

TABLE II. Mulliken loads of the heavy atoms of the studied molecules

APL L ₀	L ₁₁	L ₁₂	L ₁₃	L ₁₄	
O ₁₁ -0.806382	O ₁₁ -0.750864	O ₁₁ -0.526494	O ₁₁ -0.860038	O ₁₁ -0.828547	
O ₁₂ -0.601210	O ₁₂ -0.294258	O ₁₂ -0.619427	O ₁₂ -0.316327	O ₁₂ -0.313591	
O ₁₄ -0.677656	O ₁₄ -0.310899	O ₁₄ -0.660659	O ₁₄ -0.320893	14 O -0.307825	
O ₁₆ -0.689424	O ₁₆ -0.340576	O ₁₆ -0.649637	O ₁₆ -0.319121	15 H 0.000000	
S ₁₈ -0.230684	S ₁₈ -0.175516	S ₁₈ 0.104437	S ₁₈ -0.201040	16 O -0.359063	
N ₂₅ -0.777974	N ₂₅ -0.436045	N ₂₅ -0.543784	N ₂₅ -0.184563	18 S -0.245104	
O ₃₃ -0.667325	O ₃₃ -0.298481	O ₃₃ -0.632524	O ₃₃ -0.363602	31 O -0.360373	
O ₃₆ -0.961545	O ₃₆ -0.815511	O ₃₆ -0.479355			
N ₄₆ -0.667944	N ₄₆ -0.531620				
L ₁₅	L ₁₆	L ₁₇	L ₂₁₁	L ₂₁₂	
O ₉ -0.228212	O ₁₁ -0.375313	O ₉ -0.646524	O ₁₁ -0.806102	O ₁₁ -0.494272	
O ₁₁ -0.258525	O ₁₃ -0.360245	O ₁₁ -0.672449	O ₁₂ -0.298240	O ₁₂ -0.237619	
O ₁₃ -0.268234	S ₁₅ -0.227613	O ₁₃ -0.692649	O ₁₄ -0.326231	O ₁₄ -0.246626	
S ₁₅ 0.064980	O ₂₈ -0.402836	O ₂₃ -0.639021	O ₁₆ -0.345171	O ₁₆ -0.232486	
O ₂₈ -0.239380	O ₃₃ -0.345292	O ₂₈ -0.659311	S ₁₈ -0.159014	N ₂₀ -0.298117	
O ₃₃ -0.203297			N ₂₁ -0.635725	O ₂₈ -0.232444	
			O ₂₉ -0.282741	O ₃₁ -0.605135	
			O ₃₂ -0.879534	N ₄₁ -0.431394	
			N ₄₂ -0.647293		
L ₂₁₃	L ₂₁₄	L ₂₁₅	L ₂₂₂	L ₂₂₃	L ₂₂₄
O ₁₁ -0.485495	O ₁₁ -0.487155	O ₁₁ -0.770529	O ₁₁ -0.847370	O ₁₁ -0.516818	O ₁₁ -0.836362
O ₁₂ -0.625464	O ₁₂ -0.626757	O ₁₂ -0.323676	O ₁₂ -0.595180	O ₁₂ -0.619741	O ₁₂ -0.308736
O ₁₄ -0.654873	O ₁₄ -0.658295	O ₁₄ -0.326129	O ₁₄ -0.625393	O ₁₄ -0.659983	O ₁₄ -0.304284
O ₁₆ -0.633652	O ₁₆ -0.637287	O ₁₆ -0.315774	O ₁₆ -0.627928	O ₁₆ -0.643903	O ₁₆ -0.358326
N ₂₀ -0.547955	N ₂₀ -0.728199	O ₂₆ -0.373021	S ₁₈ -0.189657	S ₁₈ -0.066985	S ₁₈ -0.247485
O ₂₈ -0.622386	O ₂₈ -0.637626		N ₂₁ -0.670077	N ₂₁ -0.727635	O ₂₇ -0.359047
O ₃₁ -0.464787			O ₂₉ -0.587428	O ₂₉ -0.646215	
			O ₃₂ -0.749394		

According to the data in Table II, the nucleophilic centres of the molecule are S₁₈, O₃₆ and N₂₅. The probable reaction pathways determined for lincomycin

are given in Fig. 1. The hydroxyl radical, being a very active species, has a strong electrophilic character. Once it is formed, it is ready to attack the lincomycin molecule and produce reaction intermediates.

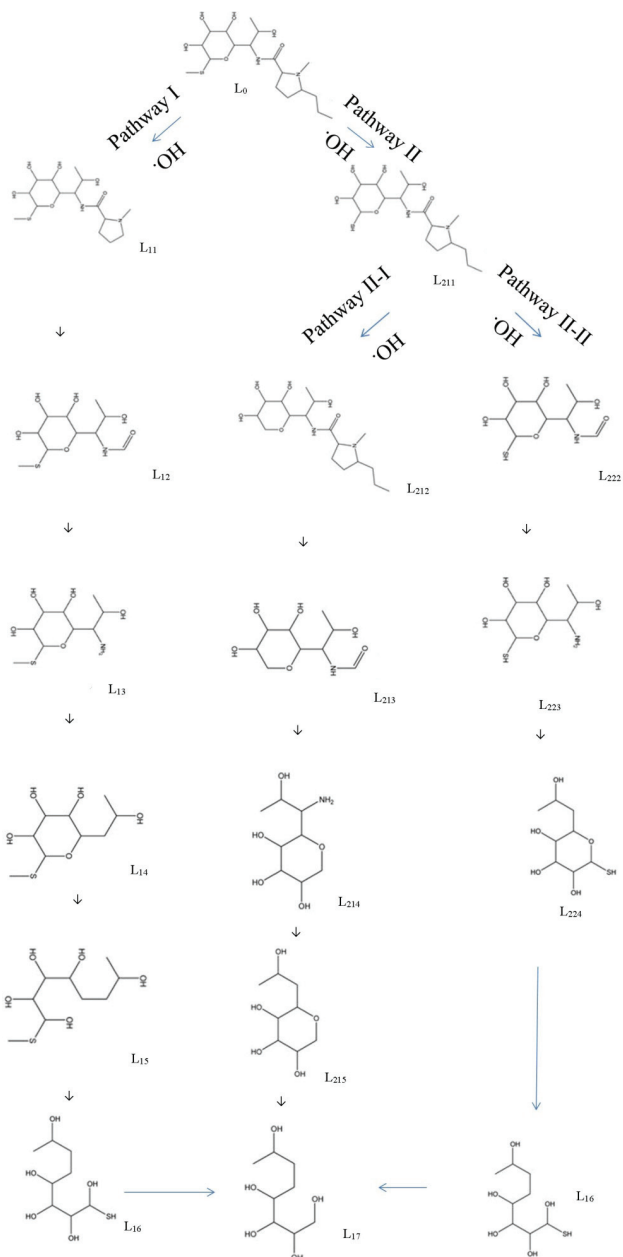


Fig. 1. The probable reaction pathways determined for lincomycin.

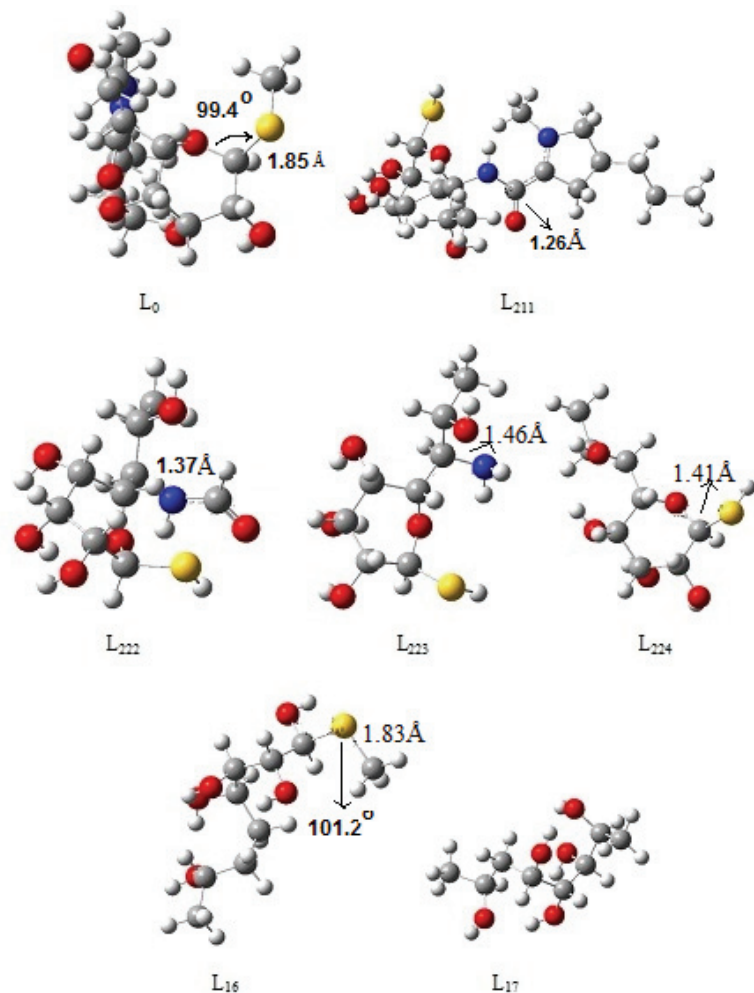


Fig. 2. The geometric shapes of L_{211} and all other fragments obtained because of optimization (grey, carbon; red, oxygen; blue, nitrogen; white, hydrogen; yellow, sulphur). (For interpretation of the references to colour in this figure legend, the reader is referred to the web version of the article).

As seen from different angles in an optimized form, lincomycin molecule (L_0) has a conformation far from a planar structure in terms of geometric shape (Fig. 2). The bond length of S atom to C atom in CH_3 group was found to be S–C 1.82742 Å, its bond length to C atom in the closed ring was found to be S–C 1.8516 Å, and the bond angle it created was determined as C–S–C 99.44260°. Bond lengths in the area of degraded L_{211} fragment were C=O 1.25848 Å, C–C 1.43762 Å, C–N 1.38830 Å; the N–C–C bond angle was 120.21676°. The subsequent fragment is L_{222} . Bond lengths in the area of the degraded L_{222} fragment

were C=O 1.22039 Å, C–H 1.10184 Å, C–N 1.37365 Å; the N–C–O bond angle was 123.20369°. The subsequent fragment is L₂₂₃. The bond lengths in the area of the degraded L₂₂₃ fragment were C–C 1.54212 Å, C–N 1.46367 Å; the N–C–O bond length was 112.96433°. The subsequent fragment is L₂₂₄. Bond lengths in the area of degraded L₂₂₄ fragment were: C–H close to the S atom 1.40810 Å, C–H 1.43116 Å; the C–O–C bond angle was 113.48227°. The subsequent fragment is L₁₆. Bond lengths in the area of the degraded L₁₆ fragment was O–H 1.40971 Å; the C–S–C bond angle was 101.28857°. The subsequent fragment is L₁₇.

CONCLUSIONS

In this study, the most probable reaction paths when an •OH is added to lincomycin were determined. When the Mulliken charges in Table II are analysed, the electronegativities of S, N and O atoms give information about the bonding state of the •OH.

Degradation reaction occurs with the attack of •OH to S. The fragment generated because of bond rupture was called L₂₁₁. The geometric shapes of L₂₁₁ and all other fragments are obtained because of optimization. The total energy of the product for gaseous phase was calculated as –1625.4413989 Ha, and for aqueous phase as –1625.4400089 Ha. The enthalpy, entropy and Gibbs energy changes calculated for both the gaseous and the aqueous phases are given in Table I. The fragment L₂₂₂ was found to be the one with the least energy in the degradation paths of the molecule, *i.e.*, the most stable fragment. This fragment is generated by bond rupture of the close ring to which the electronegative N is bound. The total energy of the product was calculated as –1257.4228785 Ha for the gaseous phase and –1257.4428949 Ha for the aqueous phase. The fragment generated because of bond rupture due to the electronegativity of N and O atoms was called L₂₂₃. The total energy of the product was calculated as –1144.0846754 Ha for the gaseous phase and –1144.0964429 Ha for the aqueous phase. The fragment generated with the separation of electronegative NH₂ group was called L₂₂₄. The energies of the formed product for the gaseous and aqueous phases were –1088.7336272 and –1088.7537095 Ha, respectively. Due to the electronegativity of the O atom in the closed ring of the formed fragment, the bond ruptured and L₁₆ fragment was formed. The energies of the formed product for the gaseous and aqueous phases were –1089.9475657 and –1089.9543748 Ha, respectively. The smallest fragment was L₁₇, which was transformed into harmless substances of the antibiotic solved in water. The total energies of the product for the gaseous and aqueous phases were calculated as –691.7740044 and –691.7684783 Ha, respectively.

As a result, degradation process requires energy. •OH are used to degrade antibiotic substances in water. As seen in the obtained fragments, lincomycin was

degraded into L₁₇ and became harmless to the environment. The aim of this study was to elucidate possible modes of lincomycin degradation mixed in water into the smallest fragment, and remove it from water resources. As also seen in the results, the degradation occurred theoretically.

Acknowledgements. The authors greatly appreciate Namik Kemal University Research Foundation for financial support. Project number: NKUBAP.00.10.AR.12.05

ИЗВОД

ИЗРАЧУНАВАЊЕ МОГУЋИХ РЕАКЦИОНИХ ПУТЕВА МОЛЕКУЛА ЛИНКОМИЦИНА
ПОМОЋУ DFT РАЧУНАРСКОГ МЕТОДА

BAHAR EREN¹ и YELDA YALCIN GURKAN²

¹Namik Kemal University, Faculty of Agriculture, Tekirdag, Turkey и ²Namik Kemal University, Department of Chemistry, Tekirdag, Turkey

Антибиотици које користе људи излучују се из тела мало или нимало промењени. Трагови елиминисаних антибиотика улазе директно у околину пошто се не могу обрадити у већини погона за третирање отпадних вода. Пораст отпорности микроорганизама може бити узрокован ниским концентрацијама трагова антибиотика док високе концентрације антибиотика могу имати токсичне ефекте. Због тога се отпадне воде које садрже трагове антибиотика морају третирати на одговарајући начин. Линкомицин је изолован из *Streptomyces lincolnensis*. Линкомицин и његови деривати су антибиотици који показују биолошку активност према грам-позитивним бактеријама. Због своје широке употребе линкомицин је природни антибиотик који се у животној околини јавља као загађивач. Ова студија тежи да предскаже механизам деградације молекула линкомицина у гасној фази и у воденој средини. Анализиран је могући пут реакције молекула линкомицина са OH радикалом. Оптимизована геометрија је нађена помоћу Gauss View 5. Затим је најнижа енергија нађена оптимизацијом са Gaussian 09 програмом. У циљу да се одреде интермедијери при фотокаталиничкој деградацији линкомицина, урађена је оптимизација методом теорије функционала густине (DFT). Израчуната је активациона енергија за могуће реакционе путеве, као и термодинамички најстабилнија стања за гасовиту и водену средину. Утицај воде као растварача истражен је коришћењем солвационог модела заклањања налик проводнику (COSMO). Предсказани механизам је потврђен поређењем са у литератури саопштеним експерименталним резултатима на простим структурима.

(Примљено 21. јула, ревидирано 21. октобра, прихваћено 8. новембра 2016)

REFERENCES

1. R .E. L. Procópio, I. R. Silva, M. K. Martins, J. L. Azevedo, J. M. Araújo, *Braz. J. Infect. Dis.* **16** (2012) 466
2. B. Halling-Sorensen, S. Nors Nielsen, P. F. Lanzky, F. Ingerslev, H. C. Holten Lützhøft, S. E. Jorgensen, *Chemosphere* **36** (1998) 357
3. T. A. Ternes, *Water Res.* **32** (1998) 3245
4. C. G. Daughton, T. A. Ternes, *Environ. Health Perspect. Suppl.* **107** (1999) 907
5. N. Kemper, *Ecol. Indic.* **8** (2008) 1
6. Y. Ohnishi, J. Ishikawa, H. Hara, *J. Bacteriol.* **190** (2008) 4050
7. D. G. Larsson, C. Pedro, N. Paxeus, *J. Hazard. Mater.* **148** (2007) 751

8. D. Li, M. Yang, J. Hu, L. Ren, Y. Zhang, H. Chang, K. Li, *Environ. Toxicol. Chem., A* **27** (2008) 80
9. D. Li, M. Yang, J. Hu, Y. Zhang, H. Chang, F. Jin, *Water Res.* **42** (2008b) 307
10. K. Kümmeler, *Chemosphere* **75** (2009) 417
11. K. V. Thomas, in *Proceedings of First International Conference on Sustainable Pharmacy*, 24–25 April, 2008, Osnabrück, Germany
12. S. E. Jorgensen, B. Halling-Sørensen, *Chemosphere* **40** (2000) 691
13. C. Winckler, A. Grafe, *Stoffeintrag durch Tierarzneimittel und pharmakologisch wirksame Futterzusatzstoffe unter besonderer Berücksichtigung von Tetrazyklinen*, UBA-Texte 44/0, Berlin, 2000
14. S. Thiele-Bruhn, *J. Plant Nutr. Soil Sci.* **166** (2000) 145
15. K. Verschueren, *Handbook of Environmental Data on Organic Chemicals*, 2nd ed., Van Nostrand Reinhold Company, New York, 1983
16. J. C. English, V. S. Bhat, G. L. Ball, C. J. McLellan, *Regul. Toxicol. Pharmacol.* **64** (2012) 269
17. R. W. Matthews, in *Photocatalytic purification and treatment of water and air*, D. F. Ollis, H. Al-Ekabi, Eds., Elsevier, New York, 1993, pp. 121–133
18. A. Taicheng, L. Sun, G. Li, S. Wan, *J. Mol., Catal., A: Chem.* **333** (2010) 128
19. V. G. Buxton, L. C. Greenstock, P. W. Helman, B. A. Ross, *J. Phys. Chem. Ref. Data* **17** (1988) 513
20. M. Anbar, P. Neta, *Int. J. Appl. Radiat. Isot.* **18** (1965) 495
21. B. Halliwell, M. Grootveld, J. M. C. Gutteridge, *Methods Biochem. Anal.* **33** (2006) 59
22. A. Hatipoglu, D. Vione, Y. Yalcin, C. Minero, Z. Cinar, *J. Photochem. Photobiol., A: Chem.* **215** (2010) 59
23. P. W. Atkins, *Physical Chemistry*, 6th ed., Oxford University Press, New York, 1998
24. K. K. Mierzejewska, J. Trylska, J. Sadlej, *J. Mol. Model.* **18** (2012) 2727
25. *Gaussian 09*, Revision B.04, Gaussian, Inc., Pittsburgh, PA, 2009
26. H. F. Diercksen, B. T. Sutcliffe, A. Veillard, in *Proceedings of the NATO Advanced Study Institute*, 4–21 September, 1974, Ramsau, Germany
27. P. W. Atkins, R. S. Friedman, *Molecular Quantum Mechanics*, 4th ed., Oxford University Press Inc., New York, 2005
28. I. N. Levine, *Quantum Chemistry*, 2nd ed., Academic Press, Waltham, MA, 1993.